High performance controllers towards ELT-sized adaptive optics systems

Léonard Prengère, Caroline Kulcsár, Henri-François Raynaud, Jean-Marc Conan

High performance controllers towards ELT-sized adaptive optics systems

Léonard Prengère[a,b,*], Caroline Kulcsár[a], Henri-François Raynaud[a], and Jean-Marc Conan[b]

[a]*Laboratoire Charles Fabry, Institut d'Optique Graduate School, 91127 Palaiseau cedex, France*
[b]*ONERA – The French Aerospace Lab, BP 72, 92322 Châtillon cedex, France*
[*]*Corresponding author: Léonard Prengère, e-mail: leonard.prengere@institutoptique.fr*

January 31, 2018

Abstract

Adaptive Optics (AO) systems compensate the nefarious effects of atmospheric turbulence affecting image formation on ground-based telescopes. Deformable Mirrors (DMs) are inserted in the telescope optical path to correct for the deformations induced by turbulence, in real-time, using Wave Front Sensor (WFS) measurements. The upcoming AO systems for ELTs (Extremely Large Telescopes) will feature a huge number of WFS measurements and DM actuators, and the design of high performance controllers adapted to these dimensions is a real challenge. In this article we compare the performance of several controllers: standard integral action, LQG (Linear Quadratic Gaussian) based on Kalman filter, and a highly parallelizable LQG based on Distributed Kalman Filter (DKF), which is built on Fourier domain models. Performance evaluation for a Single Conjugated AO (SCAO) configuration of a VLT-like telescope (8m) allows to discuss the extension to ELT-size high performance controllers.
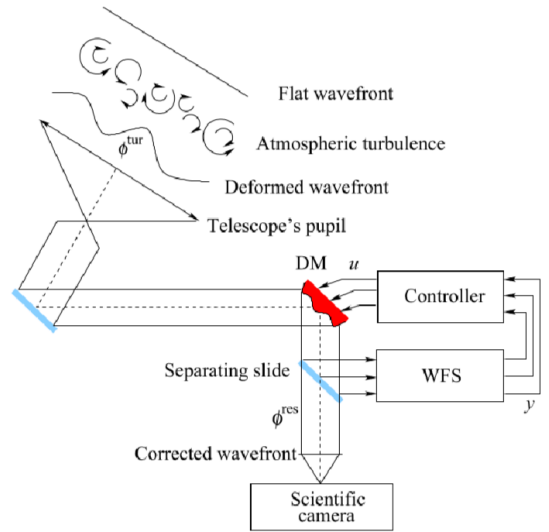
Figure 1: Principle of adaptive optics for ground-based telescopes

Figure 2: Next and previous generation telescope AO size

1 INTRODUCTION

The atmospheric turbulence introduces optical aberrations which degrade the images of astronomical objects acquired on ground-based telescopes. Adaptive Optics (AO) systems compensate these wavefront distortions using Deformable Mirrors (DMs) inserted in the telescope optical path [1]. Wavefront sensors (WFSs) provide measurements used by a real-time controller to calculate the DM commands in a control loop (Figure 1). A current generation Single Conjugated AO (SCAO, with only one DM and one WFS) system such as the Nasmyth Adaptive Optic System (NAOS) installed on the Very Large Telescope (VLT, 8m diameter) (Figure 2) has 187 controlled actuators on a 15 x 15 cartesian grid. The next generation of Extremely Large Telescopes (ELTs), currently under design and construction [2–7], features DMs with Large Degree Of Freedom (LDOF) to be controlled in real time, which is a challenge. For instance, the European-Extremely Large Telescope [5–7] features a DM with 5316 actuators.

Standard integral action regulators are used on most operational systems and thus provide a baseline for ELT AO performance. As AO systems feature control loops with delays, a high performance controller should explicitly compensate for these delays. Designing high performance controllers to fulfill the demanding requirements for ELT AO systems is even more challenging. In recent years, controllers based on turbulence models and optimal prediction (a.k.a. Linear Quadratic Gaussian (LQG) control and Kalman filter) have been proposed [8, 9]. However, a direct scaling up to ELT-sized systems is not possible with current technology. Highly parallelizable controllers have thus been proposed [10–12], but at the price of a performance degradation. Note that LQG control, and particularly the choice of dynamic models and of the type

and size of the basis for the phase description, are still active subjects of research.

In this article we analyse the performance of LQG controllers with different Auto Regressive (AR) dynamic models and different phase estimation bases. We also study an LQG controller based on a Distributed Kalman Filter (DKF) [10] which is massively parallelisable, in order to derive development directions in the framework of ELTs.

The paper is organized as follows. In section 2 we present optimal AO controllers, with AO control loop description in section 2.1, and LQG regulation in section 2.2, using Kalman filter and Distributed Kalman filter. In section 3, we analyse VLT NAOS-liked simulation results, through LQG controllers using different Auto-Regressive dynamical models in section 3.1, with different spatial resolution in section 3.2, and a Distributed Kalman filter-based control in section 3.3. Then we conclude this study by proposing development directions towards high performance control for ELT-scaled AO systems.

2 Optimal controllers

2.1 AO control loop

An AO system can be represented by a discrete-time block diagram (Figure 4) where all blocks are linear operators. The incoming perturbation is the turbulent phase ϕ^{tur}, ϕ^{cor} is the correction phase generated by the DM and ϕ^{res} is the residual phase. The WFS delivers noisy wavefront measurements y where w represents the noise measurement. The DM commands u are computed by the controller from the wavefront measurements. In this control loop we have delays introduced by the control and measurement computations, and by the integration and readout time of the WFS camera. We approximate the total loop delay by two frames. The standard controller used
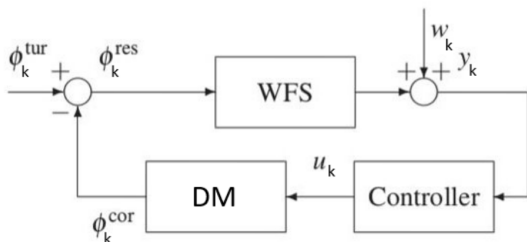

Figure 3: AO control loop block diagram

on most operational systems in SCAO mode is an integral action regulator in the form:

$$u_k = u_{k-1} + GM_{com}y_k, \qquad (1)$$

where M_{com} is the command matrix, *i.e.* the generalized inverse of the DM to WFS interaction matrix DN (see below), and G is a scalar gain. In order to have a stable closed-loop system in this two-frame delay case, the gain G should satisfy $0 \le G < 1$. Predictive control can be used to counteract the effect of delays. In the case of AO the optimal solution to the minimisation of the residual phase variance is obtained with LQG control [13], as soon as a linear stochastic dynamical model of the turbulent phase can be established, and if all noises are Gaussian.

LQG control is based on a Kalman filter that predicts the turbulent phase.

2.2 LQG regulation

2.2.1 Quadratic performance criterion

The LQG regulator is optimal in the sense of the residual phase variance $\sigma^2_{\phi_{\mathrm{res}}}$ defined as

$$\sigma^2_{\phi^{\mathrm{res}}} = \lim_{n\to\infty} \frac{1}{n} \sum_{k=0}^{n-1} \|\phi_k^{\mathrm{res}}\|^2 = \lim_{n\to\infty} \frac{1}{n} \sum_{k=0}^{n-1} \|\phi_k^{\mathrm{tur}} - \phi_k^{\mathrm{cor}}\|^2. \qquad (2)$$

If the DM has no temporal dynamics and a linear response, with influence matrix N, the correction phase at time k is given by:

$$\phi_k^{\mathrm{cor}} = Nu_{k-1} \qquad (3)$$

and the optimal control that minimizes $\sigma^2_{\phi_{\mathrm{res}}}$, under the unrealistic assumption that future values $\phi_{k+1}^{\mathrm{tur}}$ of the turbulence are known (the so-called "complete information" hypothesis), is

$$u_k = (N^tN)^{-1}N^t\phi_{k+1}^{\mathrm{tur}}. \qquad (4)$$

When the turbulent phase $\phi_{k+1}^{\mathrm{tur}}$ is unknown (in so-called "incomplete information"), the stochastic separation theorem applies and the optimal control is simply obtained by replacing $\phi_{k+1}^{\mathrm{tur}}$ in (4) by its optimal estimate, in the sense of minimum estimation error variance, $\hat{\phi}_{k+1|k}^{\mathrm{tur}} = \mathrm{E}(\phi_{k+1}|\mathfrak{I}_k)$, to finally get

$$u_k = (N^tN)^{-1}N^t\hat{\phi}_{k+1|k}^{\mathrm{tur}}. \qquad (5)$$

The set $\mathfrak{I}_k$ represents all the information until time k. The predicted phase $\hat{\phi}_{k+1|k}^{\mathrm{tur}}$ is obtained as the output of a Kalman filter (see [14] for more information on minimum variance control in AO).

2.2.2 Kalman filter

The Kalman filter is based on a stochastic model of the turbulent phase temporal evolution. For instance, in the case of an Auto-Regressive model of order 2 (AR2), we have

$$\phi_{k+1} = A_1\phi_k + A_2\phi_{k-1} + v_k, \qquad (6)$$

where A_1 and A_2 are matrix coefficients, and v is a Gaussian white noise with known covariance matrix Σ_v. The state equation

$$x_{k+1} = Ax_k + V_k, \qquad (7)$$

is equivalent to (6), with $A = \begin{pmatrix} A_1 & A_2 \\ I & 0 \end{pmatrix}$, $V_k = \begin{pmatrix} v_k \\ 0 \end{pmatrix}$, and with the state vector x_k defined as

$$x_k = \begin{pmatrix} \phi_k^{\mathrm{tur}} \\ \phi_{k-1}^{\mathrm{tur}} \end{pmatrix}. \qquad (8)$$

Taking $C = \begin{pmatrix} 0 & D \end{pmatrix}$, the measurement equation $y_k = D\phi_{k-1} + w_k - DNu_{k-2}$ becomes

$$y_k = Cx_k + w_k - DNu_{k-2}, \qquad (9)$$

where D is the WFS matrix model, and w is a Gaussian white noise with known covariance matrix Σ_w. This state

space representation leads to the asymptotic Kalman filter in prediction form

$$\hat{x}_{k+1|k} = A\hat{x}_{k|k-1} + L_\infty(y_k - \hat{y}_{k|k-1}), \qquad (10)$$

that is computed in real-time. The prediction Kalman gain L_∞, defined as

$$L_\infty = A\Sigma_\infty C^t (C\Sigma_\infty C^t + \Sigma_w)^{-1}, \qquad (11)$$

is to be computed off-line. The asymptotic estimation error covariance matrix Σ_∞ is obtained as the solution of a Discrete Algebric Riccati Equation (DARE):

$$\Sigma_\infty = A\Sigma_\infty A^t + \Sigma_V - A\Sigma_\infty C^t (C\Sigma_\infty C^t + \Sigma_w)^{-1} C\Sigma_\infty A^t. \qquad (12)$$

At last, $\hat{y}_{k|k-1} = \mathrm{E}(y_k|\mathfrak{I}_{k-1})$ is the predicted measurement and is obtained as

$$\hat{y}_{k|k-1} = C\hat{x}_{k|k-1} - DNu_{k-2}. \qquad (13)$$

The predicted turbulent phase is finally obtained from the predicted state vector

$$\hat{\phi}_{k+1|k} = C_\phi \hat{x}_{k+1|k}, \qquad (14)$$

where $C_\phi = \begin{pmatrix} I & 0 \end{pmatrix}$. The predicted phase $\hat{\phi}_{k+1|k}$ can be expressed in different bases e.g., a modal basis like the Zernike basis, or a zonal basis (spatial sampling of the phase in the telescope pupil plane), or a Fourier basis with spatial frequencies. The control performance is impacted by the accuracy of the phase description: for instance, the number of modes in a modal basis [9] or the sampling for a zonal basis [11]. However an improvement of the phase description accuracy increases the computation time of the DARE (12), the Kalman gain L_∞ in (11), and of the predictive equation (13). The basis dimension is thus a real question for ELT-scaled AO systems.

The standard version of the Kalman filter proves to be impractical in terms of implementation for LDOF AO systems, like ELTs, because of excessive cost to solve the DARE and to perform the operations in (10). Several approaches have been proposed to overcome this computationnal bottleneck [15–18]. One of them is the Distributed Kalman Filter (DKF) which was proposed for a large scale wide-field AO system [10, 11], with application to the Thirty Meter Telescope [11]. The DKF is a suboptimal approach that is highly parallelizable.

2.2.3 Distributed Kalman Filter

This filter proposed in [10] is based on phases described in a zonal basis, and is built on an infinite pupil hypothesis, which means that the spatial support of the measurements and estimated phases is supposed to be infinite. It follows from these asumptions that the state equation (7), the measurement equation (9) and the prediction equation (10) become spatially invariant and can be expressed as convolution products:

$$x_{k+1} = A * x_k + V_k, \qquad (15)$$

$$y_k = C * x_k + w_k - (DN) * u_{k-2}, \qquad (16)$$

$$\hat{x}_{k+1|k} = A * \hat{x}_{k|k-1} + L_\infty^{DKF} * (y_k - \hat{y}_{k|k-1}). \qquad (17)$$

Convolution products are highly parallelizable and this allows to reduce the computational time of the Kalman filter prediction equation. Moreover using a convolution kernel as Kalman gain makes it possible to reduce the kernel size without affecting significantly the control performance [10]. Indeed, as illustrated in Figure 4, the Kalman gain kernel is well localized. The spatial invariance prop-
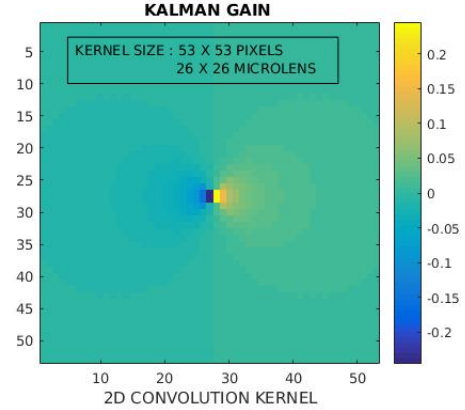

Figure 4: Example of Kalman gain kernel for DKF

erty allows an efficient evaluation of the Kalman gain kernel L_∞^{DKF} in Fourier basis where each gain value associated with a 2D spatial frequency is independent from the others (decoupled spatial frequencies). In the case of a monolayer AR1 phase model, the phase estimation error covariance matrix in Fourier space $\tilde{\Sigma}_\infty$ can be computed for each spatial frequency pair (ν_x, ν_y) with a 2nd degree polynomial scalar equation

$$\begin{aligned} \tilde{\Sigma}_{\infty_{\nu_x,\nu_y}} = & |\tilde{A}_{\nu_x,\nu_y}|^2 \tilde{\Sigma}_{\infty_{\nu_x,\nu_y}} + \tilde{\Sigma}_{V_{\nu_x,\nu_y}} - |\tilde{A}_{\nu_x,\nu_y}|^2 \\ & (\tilde{\Sigma}_{\infty_{\nu_x,\nu_y}})^2 \tilde{C}_{\nu_x,\nu_y}^H (\tilde{C}_{\nu_x,\nu_y} \tilde{C}_{\nu_x,\nu_y}^H \tilde{\Sigma}_{\infty_{\nu_x,\nu_y}} \\ & + \sigma_w^2 I)^{-1} \tilde{C}_{\nu_x,\nu_y}, \end{aligned} \qquad (18)$$

where $\tilde{A}, \tilde{C}$ are the Fourier representation of A, C respectively in the state model (15, 16), σ_w^2 is the measurement noise variance and $\tilde{\Sigma}_V$ is the Fourier space covariance matrix of the noise V in (15) (for more details see [12]). The Kalman gain in Fourier space is computed from $\tilde{\Sigma}_\infty$ for each 2D spatial frequency with

$$\begin{aligned} \tilde{L}_{\infty_{\nu_x,\nu_y}}^{DKF} = & \tilde{A}_{\nu_x,\nu_y} \tilde{\Sigma}_{\infty_{\nu_x,\nu_y}} \tilde{C}_{\nu_x,\nu_y}^H (\tilde{C}_{\nu_x,\nu_y} \tilde{C}_{\nu_x,\nu_y}^H \tilde{\Sigma}_{\infty_{\nu_x,\nu_y}} \\ & + \sigma_w^2 I)^{-1} \tilde{C}_{\nu_x,\nu_y}, \end{aligned} \qquad (19)$$

before coming back in zonal base with a 2D inverse Fourier transform.

3 Simulation results

We simulate a VLT NAOS-like case with a three layer atmosphere with respectively a windspeed of 7.5, 12.5, and 15 m/s, and a direction of 0,120 and 240°. The overall Fried diameter [1] is 10 cm at 0.55 μm, with a relative energy repartition per layer of 0.5, 0.17 and 0.33. The WFS is a Shack-Hartmann, and the DM is in Fried geometry, where the actuators are located at the corners of the Shack-Hartmann subapertures, if we represent the actuator grid in the WFS plane. We consider here a 15 x 15 actuator grid (187 actuators are controlled), and a

14 x 14 subaperture grid with 152 valid subapertures. In our simulations the WFS camera wavelength is 0.55 μm, the WFS measurement noise is 0.2 rad^2 and the scientific image camera wavelength is 1.65 μm (H band of the atmosphere). All simulations presented in this paper have been performed with the tool Object Oriented Matlab Adaptive Optics (OOMAO).

The AR1 dynamic model used for LQG design, is a simple diagonal model where

$$A = \alpha I, \tag{20}$$

and

$$\phi_{k+1} = A\phi_k + v_k. \tag{21}$$

The AR2 dynamic model (6) is here defined in a Zernike basis, as described and tested on sky on CANARY in [19].

3.1 Dynamic Model in LQG

We first analyse the performance of LQG and integral action regulators. We evaluate LQG controllers with a phase estimated in a modal Zernike basis of 495 modes, with the two different AR models mentioned above. Performance is given in terms of Strehl Ratio (SR), at 1.65 μm, which is an image quality metric (100 % corresponds to the diffraction limited case). In our simulation we use the approximation $SR = \exp(-\sigma^2_{\phi_{\mathrm{res}}})$ [20] where $\sigma^2_{\phi_{\mathrm{res}}}$ is the residual phase variance at the imaging wavelength.

Control	Model	Strehl Ratio
Standard Integral control	/	51.2 %
LQG	AR1	51.0 %
LQG	AR2	54.2 %

Table 1: Control Performance with LQG and integral action regulators

The LQG regulator with an AR2 model clearly outperforms the standard integral controller (Table 1) in SCAO mode. Note that the simpler AR1 model is however not sufficient to gain in performance.

3.2 Spatial resolution

The estimator $\hat{\phi}^{\mathrm{tur}}_{k+1|k}$ can be expressed in many bases, and the control performance is strongly impacted by the size of the bases. In this part we study the evolution of performance when we increase the number of modes of a Zernike basis, and the number of points of a zonal basis.

3.2.1 Zernike basis: influence of the number of modes

For instance, for Zernike modal basis we show improvement (Table 2) when using more modes, for both AR1

Number of modes	Model	Strehl Ratio
189 modes	AR1	42.2 %
495 modes	AR1	51.0 %
189 modes	AR2	44.8 %
495 modes	AR2	54.1 %

Table 2: Performance of LQG regulators using Zernike basis in a VLT NAOS-like simulation case

and AR2 dynamic models.

3.2.2 Zonal basis: influence of the spatial sampling

To give an idea of the impact of the 2D sampling, we have used different sampling periods to spatially represent the phase. Different sampling periods are obtained by modifying the number of sampling points in a WFS subaperture area. For the phase illustrated in Figure 5, we have computed in Figure 6 its predicted value, as obtained by the Kalman filter, with various sampling periods. A better sampling (between 1 and 4 points per subaperture) of the predicted phase clearly improves LQG performance, as shown in Table 3. Indeed, having 4
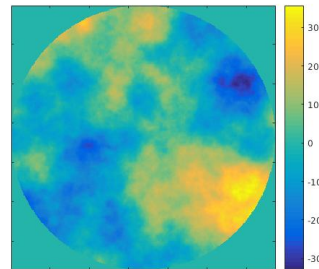

Figure 5: Turbulent phase screen on a VLT-like simulation
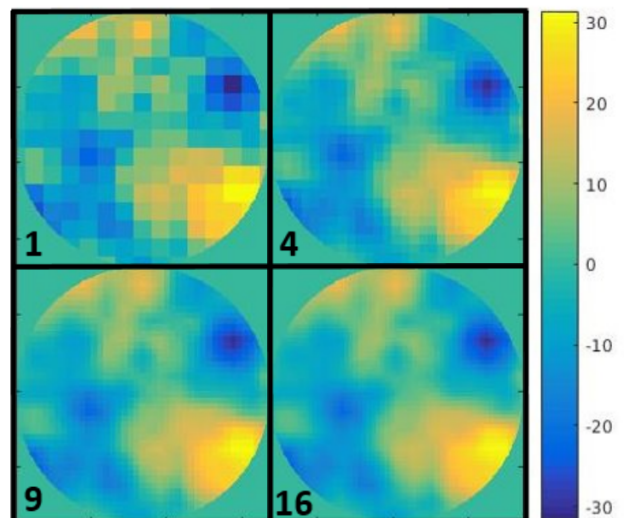

Figure 6: Predicted phase screens depending on the zonal base sampling (1, 4, 9 or 16 points per subaperture area)

points per subaperture in the predicted phase improves the estimation quality and gives a better representation of the spatial frequencies that the DM can correct. The

Sampling of subaperture	Strehl Ratio
1 point / subaperture	42.2 %
4 points / subaperture	50.3 %
9 points / subaperture	50.7 %
16 points / subaperture	51.5 %

Table 3: Performance of LQG regulator using an AR1 dynamic model and estimate phases $\hat{\phi}^{\mathrm{tur}}_{k+1|k}$ in zonal bases

atmospheric turbulence contains very high spatial frequencies [1], that are beyond WFS Nyquist spatial frequency. The Shack-Hartmann WFS thus introduces aliasing effects on the wavefront measurements, that the Kalman filter

can partially unfold by estimating the phase with statistical priors, on a finer grid than the WFS subaperture grid. However, we only have marginal improvements from 4 points to 16 points per WFS subaperture. The aliasing unfolding is probably limited by the crudeness of the AR1 dynamic turbulent phase model.

3.3 DKF performance & limitations

The DKF is a highly parallelizable filter, which evaluates the prediction equation much faster than the standard Kalman Filter as defined in equation (10). We compare two LQG regulators performance, one with standard Kalman filter (KF-based control) and the other with a DKF (DKF-based control), both using an AR1 dynamic model (20, 21). As a standard KF-based control, the

Sampling of one WFS subaperture	DKF-based control	KF-based control
1 point / subaperture	41.9 %	42.2 %
4 points / subaperture	47.5 %	50.3 %

Table 4: Performance of LQG regulators, based on Kalman filter and DKF, both using a zonal AR1 dynamic model

DKF-based control is sensitive to the discretization of the zonal basis (Table 4). Nevertheless there is a performance decrease of the DKF-based controller with respect to the KF-based control, particularly for the 4 points per subaperture case. The infinite pupil hypothesis may cause this degradation. Indeed, although rather valid at the center of the pupil, it is less relevant at the edges.

4 CONCLUSION

In this paper, we analyze the performance of model-based AO controllers, evaluated on a VLT-like SCAO system. We study different LQG regulators, based on either a Kalman filter or on a distributed Kalman filter, in order to guide future developments for ELT-sized AO. We first consider LQG controllers based on Kalman filters with two different AR models. As expected, a more accurate dynamical model of the turbulent phase allows LQG to outperform standard integral action control. Then we analyze phase description bases and show that a modal basis with more Zernike modes or a zonal basis with a finer sampling improves LQG performance. In the case of the DKF, an oversampling is acceptable in terms of computational time because of its highly parallelizable structure well adapted to ELT-sized AO systems. However, we show that the DKF leads to lower control performance than the standard Kalman filter. This performance degradation is mainly located at the telescope pupil edges, and is thus probably due to the infinite pupil hypothesis. We envision two actions to overcome the current limitations of the DKF. First, we need to design more accurate AR models of the turbulent phase in zonal basis in order to increase control performance for all model-based controllers. Then, using this new modeling, a so-called "hybrid" controller can be designed, where the DKF-based controller

is used inside the telescope pupil and another controller is in charge of the actuators located close to the edges.

5 ACKNOWLEDGEMENTS

References

[1] F. Roddier, *Adaptive optics in astronomy*, Cambridge university press (1999).

[2] G. Herriot, D. Andersen, J. Atwood, C. Boyer, P. Byrnes, K. Caputa, B. Ellerbroek, L. Gilles, A. Hill, Z. Ljusic, J. Pazder, M. Rosensteiner, M. Smith, P. Spano, K. Szeto, J.-P. Véran, I. Wevers, L. Wang et R. Wooff, *NFIRAOS: first facility AO system for the Thirty Meter Telescope*, Proc. SPIE, 9148, pp. 914810–914810–11 (2014).

[3] A. H. Bouchez, D. S. Acton, R. Biasi, R. Conan, B. Espeland, S. Esposito, J. Filgueira, D. Gallieni, B. A. McLeod, E. Pinna et al., *The Giant Magellan telescope adaptive optics program*, Dans *Adaptive Optics Systems IV*, vol. 9148, p. 91480W. International Society for Optics and Photonics (2014).

[4] E. Diolaiti, C. Arcidiacono, G. Bregoli, R. C. Butler, M. Lombini, L. Schreiber, A. Baruffolo, A. Basden, M. Bellazzini, E. Cascone et al., *Preparing for the phase B of the E-ELT MCAO module project*, Dans *Adaptive Optics Systems IV*, vol. 9148, p. 91480Y. International Society for Optics and Photonics (2014).

[5] Y. Clénet, T. Buey, G. Rousset, E. Gendron, S. Esposito, Z. Hubert, L. Busoni, M. Cohen, A. Riccardi, F. Chapron et al., *Joint MICADO-MAORY SCAO mode: specifications, prototyping, simulations and preliminary design*, Dans *Adaptive Optics Systems V*, vol. 9909, p. 99090A. International Society for Optics and Photonics (2016).

[6] N. A. Thatte, F. Clarke, I. Bryson, H. Schnetler, M. Tecza, R. M. Bacon, A. Remillieux, E. Mediavilla, J. M. H. Linares, S. Arribas et al., *HARMONI: the first light integral field spectrograph for the E-ELT*, Dans *Ground-based and Airborne Instrumentation for Astronomy V*, vol. 9147, p. 914725. International Society for Optics and Photonics (2014).

[7] B. Neichel, T. Fusco, J.-F. Sauvage, C. Correia, K. Dohlen, K. El-Hadi, L. Blanco, N. Schwartz, F. Clarke, N. Thatte et al., *The adaptive optics modes for HARMONI: from Classical to Laser Assisted Tomographic AO*, Dans *Adaptive Optics Systems V*,

vol. 9909, p. 990909. International Society for Optics and Photonics (2016).

[8] B. Le Roux, C. Kulcsár, L. M. Mugnier, T. Fusco, H.-F. Raynaud et J.-M. Conan, *Optimal control law for classical and multiconjugate adaptive optics*, JOSA A, 21 (7), pp. 1261–1276 (2004).

[9] C. Petit, J.-M. Conan, C. Kulcsár et H.-F. Raynaud, *Linear quadratic Gaussian control for adaptive optics and multiconjugate adaptive optics: experimental and numerical analysis*, J. Opt. Soc. Am. A, 26 (6), pp. 1307–1325 (Jun 2009).

[10] P. Massioni, C. Kulcsár, H.-F. Raynaud et J.-M. Conan, *Fast computation of an optimal controller for large-scale adaptive optics*, J. Opt. Soc. Am. A, 28 (11), pp. 2298–2309 (Nov 2011).

[11] L. Gilles, P. Massioni, C. Kulcsár, H.-F. Raynaud et B. Ellerbroek, *Distributed Kalman filtering compared to Fourier domain preconditioned conjugate gradient for laser guide star tomography on extremely large telescopes*, JOSA A, 30 (5), pp. 898–909 (2013).

[12] P. Massioni, L. Gilles et B. Ellerbroek, *Adaptive distributed Kalman filtering with wind estimation for astronomical adaptive optics*, JOSA A, 32 (12), pp. 2353–2364 (2015).

[13] C. Kulcsár, H.-F. Raynaud, C. Petit, J.-M. Conan et P. V. de Lesegno, *Optimal control, observers and integrators in adaptive optics*, Optics express, 14 (17), pp. 7464–7476 (2006).

[14] C. Kulcsár, H.-F. Raynaud, C. Petit et J.-M. Conan, *Minimum variance prediction and control for adaptive optics*, Automatica, pp. 1939–1954 (septembre 2012).

[15] A. Beghi, A. Cenedese et A. Masiero, *On the computation of Kalman gain in large adaptive optics systems*, Dans *Control & Automation (MED), 2013 21st Mediterranean Conference on*, pp. 1374–1379. IEEE (2013).

[16] C. Correia, J.-M. Conan, C. Kulcsár, H.-F. Raynaud et C. Petit, *Adapting optimal LQG methods to ELT-sized AO systems*, Dans *1st AO4ELT conference-Adaptive Optics for Extremely Large Telescopes*, p. 07003. EDP Sciences (2010).

[17] P. Massioni et M. Di Loreto, *Fast finite-horizon Kalman filter in wavefront estimation for adaptive optics*, Dans *Control Conference (ECC), 2014 European*, pp. 2398–2403. IEEE (2014).

[18] P. Massioni, H.-F. Raynaud, C. Kulcsár et J.-M. Conan, *An approximation of the Riccati equation in large-scale systems with application to adaptive optics*, IEEE Transactions on Control Systems Technology, 23 (2), pp. 479–487 (2015).

[19] G. Sivo, C. Kulcsár, J.-M. Conan, H.-F. Raynaud, E. Gendron, A. Basden, F. Vidal, T. Morris, S. Meimon, C. Petit, D. Gratadour, O. Martin, Z. Hubert, A. Sevin, D. Perret, F. Chemla, G. Rousset, N. Dipper, G. Talbot, E. Younger, R. Myers, D. Henry, S. Todd, D. Atkinson, C. Dickson et A. Longmore, *First on-sky SCAO validation of full LQG control with vibration mitigation on the CANARY pathfinder*, Optics Express, 22, pp. 23565–23591 (2014).

[20] V. N. Mahajan, *Strehl ratio for primary aberrations in terms of their aberration variance*, J. Opt. Soc. Am., 73 (6), pp. 860–861 (Jun 1983).